Advanced Composite Materials

ISSN: 0924-3046 (Print) 1568-5519 (Online) Journal homepage: http://www.tandfonline.com/loi/tacm20

A study on aerodynamic and structural design of high efficiency composite blade of 1 MW class HAWTS considering fatigue life

Changduk Kong, Minwoong Kim & Gilsu Park

To cite this article: Changduk Kong, Minwoong Kim & Gilsu Park (2015) A study on aerodynamic and structural design of high efficiency composite blade of 1 MW class HAWTS considering fatigue life, Advanced Composite Materials, 24:1, 67-83, DOI: 10.1080/09243046.2014.881630

To link to this article: http://dx.doi.org/10.1080/09243046.2014.881630

Advanced Composite Materials, 2015
Vol. 24, No. 1, 67–83, http://dx.doi.org/10.1080/09243046.2014.881630

A study on aerodynamic and structural design of high efficiency composite blade of 1 MW class HAWTS considering fatigue life

Changduk Kong*, Minwoong Kim and Gilsu Park

Department of Aerospace Engineering, Chosun University, 375 Seosuk-dong Dong-gu, Gwangju 501-759, Republic of Korea

(*Received 9 January 2013; accepted 7 January 2014*)

In this work, 1 MW class horizontal axis wind turbine blade configuration is properly sized and analyzed using the newly proposed aerodynamic design procedure and the in-house code developed by authors, and its design results are verified through comparison with experimental results of the previously developed wind turbine blade. The wind turbine structural design is carried out using the glass/epoxy composite materials and the simplified deign methods by the netting rule and the rule of mixture. The structural safety of the designed blade structure is investigated through the various load case studies, and stress, deformation, buckling, and vibration analyses using a commercial FEM code, MSC.NASTRAN. Finally, the required 20 years fatigue life is confirmed using the modified Spera's empirical formulae.

Keywords: HAWTS (Horizontal Axis Wind Turbine System); glass/epoxy composite materials; aerodynamic design; structural design; fatigue life

1. Introduction

There is increased concern recently regarding energy crisis and environmental issues due to the excessive consumption of fossil fuel are being faced. To overcome the difficulty, the wind power has risen as an important renewable energy source. The recent trend of the wind turbine system development has become much larger scale, such as 3–5 MW classes developed and commercialized by Vestas, Enercon, Repower, GE wind, etc. during past 10 years. Very recently, more than 6 MW classes are under development.[1] According to literature survey on designs, Grujicic et al. studied on structural design of 1 MW class horizontal axis wind turbine system (HAWTS),[2] and Pengwen Sun et al. studied on structural analysis of four types of layered laminate 1 MW class HAWTS patterns of 1.2 MW class HAWTS blade.[3] In Korea 750, 2, and 3 MW class wind turbines were developed completely in the early 1990s, and now 5 MW class wind turbine is developed.[4]

The reason why fatigue requirement often drives the design of the primary structural members of a wind turbine is that wind turbines must achieve very long operating lives of 20–30 years for cost effectiveness. Fatigue life is usually expressed by the term cycles to failure, which is the number of repetitions of significant loads that can be sustained from beginning until growing cracks to an allowable length.[5]

For fatigue design, allowable fatigue stress should be obtained from standard laboratory tests of the materials of construction. There are two general methods to

*Corresponding author. Email: cdgong@chosun.ac.kr

account for the stress spectrum effect, which is the first step needed to modify laboratory test data into fatigue allowable stresses.

Palmgren [6] and Miner [7] proposed the linear damage hypothesis that the stress cycle remains constant throughout a fatigue lifetime equal to N, and then the fraction of that lifetime consumed on every cycle is constant and equal to $1/N$. Mandel et al. [8] found the S–N data, which were expressed as a power law equation, in mostly unidirectional glass fiber composites.

Veers et al. [9] proposed a computer program FAROW that evaluates the fatigue and reliability of wind turbine components using structural reliability methods. Bishop et al. [10] showed a fatigue analysis of wind turbine blades using frequency domain techniques. A fracture mechanics model for fatigue damage process was proposed by Broek [11], Tada et al. [12], Suresh [13], and Finger [14]. Spera [5] proposed the experimental equations to estimate the fatigue life of 2.5 MW class wind turbine NASA/DOE Mod-2's blade using the load spectrum data, and Kong et al. [15,16] proposed the modified Spera's method to estimate the fatigue life of the 750 KW class horizontal wind turbine blade.

In order to establish the light weight design procedure considering fatigue life, this study proposes newly a design procedure on both aerodynamic and structural design procedures of more efficiency and lightweight E-glass/epoxy composite wind turbine blade of a 1 MW class HAWTS than the existing same class wind turbine blades. To validate the proposed aerodynamic design method, the design and performance analysis results using the proposed design procedure are compared to experimental test results of 900 W class Whisper H40 wind turbine which was tested by Appalachian State University in USA.

The structural design is carried out using the simplified design methods such as netting rule and rule of mixture and low-cost glass/epoxy skin and spar-urethane foam sandwich composite materials. Moreover, the parametric studies are carried out to find an acceptable blade structural design, and then the proper design parameter values are decided.

To evaluate the designed composite wind turbine blade, both the performance and structural analyses are performed using the in-house code and a commercial finite element code, MSC.NSATRAN.

An acceptable wind turbine blade, which satisfies the design requirements including the required aerodynamic power and the structural safety under various load conditions, is finally proposed.

2. Aerodynamic design of blade

To design a target wind turbine system, the design requirement must be established through existing market survey, design data base, and customer need. Table 1 shows the system design requirements for 1MW HAWTS to be designed in this work.

The diameter of the wind turbine is initially determined from the following two equations on the power.[17]

$$P_{\max} = 0.37AV^3 \tag{1}$$

$$P = 0.2D^2V^3 \tag{2}$$

where $P_{\max}$ is the maximum power by Betz theory, P is the power of the fast wind turbine, A is the swept area of blade, V is the rated wind speed, and D is the diameter of blade.

Table 1. Design requirements of wind turbine system.

Type	Horizontal axis wind turbine system (HAWTS)
Rated power	1 MW
Working range	Cut-in wind speed: less than 3 m/s Rated wind speed: 12 m/s Cut-out wind speed: 25 m/s Max. survival wind speed: 55 m/s
Number of blades	3
Tip speed ratio	7

In the next step, the blade configuration parameters such as chord length, airfoil and twisting angle, and tip speed ratio are determined from the design requirements such as rated wind speed and max tip speed ratio. After initial sizing, the first design is repeatedly modified until the required power through aerodynamic analysis using CFD tool and experimental test is obtained.

In this work, the design is carried out by the following way. Firstly aerodynamic design parameters such as the function θ of tip speed parameter λ, rotational wind speed ratio h, and axial wind speed ratio k are defined as:

$$h = (\pi + \tan^{-1}\lambda)/3 \tag{3}$$

$$k = \sqrt{\lambda^2 + 1}\cos\theta \tag{4}$$

$$h = \sqrt{1 + (1 - k^2)/\lambda^2} \tag{5}$$

Therefore, the twisting α can be calculated by the following equation:

$$\lambda_e = \lambda \frac{1 + h}{1 + k} = \cot i \tag{6}$$

$$\alpha = I - i \tag{7}$$

where I is the inclination angle, i is the incidence angle, and λ is the tip speed ratio. According to calculation results, the maximum twisting angle is 24.687°. The blade chord length l can be calculated by the following equation:

$$l = \frac{8\pi r(1 - k)}{C_l b(1 + k)\lambda_e \sqrt{\lambda_e^2 + 1}} \tag{8}$$

The aerodynamic analysis is performed to confirm the design and performance requirements of the designed wind turbine blade.[18]

Therefore, thrust coefficient C_F, moment coefficient C_M, and power coefficient C_P are calculated by the following equations:

$$C_F = 2\int_0^1 (1 - k^2)\frac{r}{R} d\left(\frac{r}{R}\right) \tag{9}$$

$$C_M = 2\int_0^1 \lambda(1 + k)(h - 1)\frac{r^2}{R^2} d\left(\frac{r^2}{R^2}\right) \tag{10}$$

$$C_P = C_M \times \lambda_0 \quad (11)$$

Aerodynamic power P and electrical power P_e can be calculated by the following equations:

$$P = \frac{1}{2}\rho C_P S V^3 \quad (12)$$

$$P_e = \eta_0 \times P \quad (13)$$

Using the equations mentioned above, the in-house code 'HAWTBAD' is developed.

At the beginning of design, the proper selection of the wind turbine blade airfoil shape is very important to design a better performance wind turbine system. In general, the criteria for selecting the airfoil are as follows: the airfoil must have following characteristics, such as less lift change during Reynolds number change, high maximum lift coefficient and stall angle of attack, high lift-drag ratio, and thicker airfoil for structural strength. In addition, the variable pitch type wind turbine uses an airfoil having high power coefficient change at a small pitch angle change.

Based on this airfoil selection criteria, this work selects the blade airfoil of NACA 63-421 through comparison of maximum lift coefficient, lift-drag ratio, and blade thickness of various airfoils referred to wind turbine airfoil catalog. Figure 1 shows the geometric configuration and the light and drag coefficients vs. angle of attack.[19]

The aerodynamic design scheme is a way to get an optimum twisting angle for a maximum lift-drag coefficient at each spanwise blade station. Figure 2 shows the aerodynamic configuration design result of 1 MW class wind turbine blade.

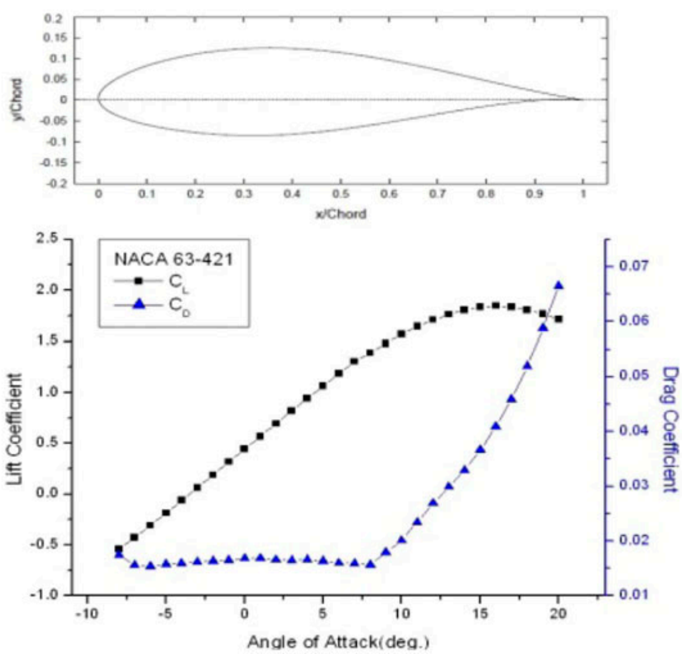

Figure 1. Airfoil configuration and aerodynamic performance characteristics.

Figure 2. Aerodynamic configuration design result of 1 MW lass wind turbine blade.

The performance analysis result of the designed wind turbine blade shows to produce much higher power than the power requirement. Moreover, it has much higher power coefficient than the existing wind turbine blade's power coefficient at rated wind speed. Figure 3 shows comparison results of power coefficient between the designed 1 MW wind turbine blade and the existing 1 MW E-44 ENERCON wind turbine blade. The comparison shows that the designed blade has better efficiency than the existing blade's efficiency at the rated wind speed.

To evaluate the proposed in-house code HAWTBAD, experimental test data of the 900 W class Whisper H40 wind turbine developed by Appalachian State University are

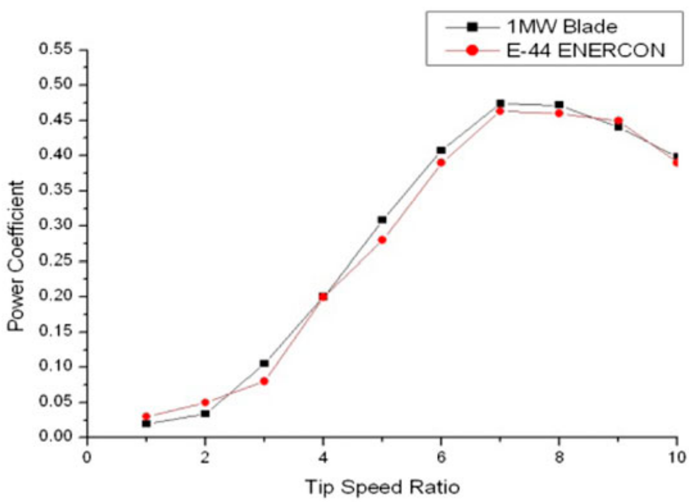

Figure 3. Comparison of power coefficient between the designed 1 MW wind turbine blade and the existing 1 MW E-44 ENERCON wind turbine blade.

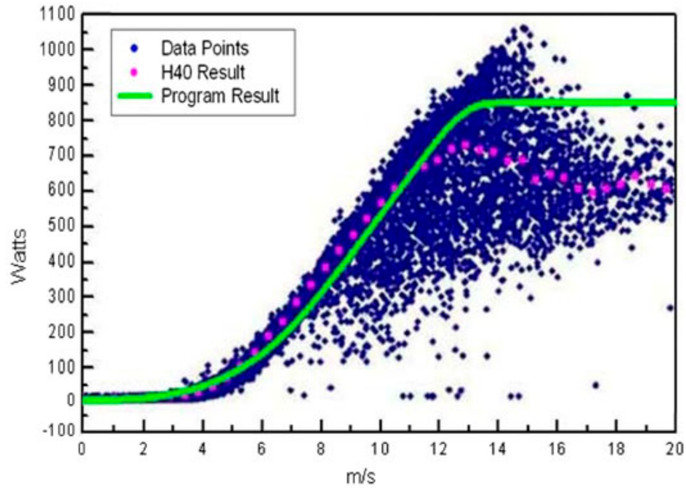

Figure 4. Comparison between Whisper H40's test results and performance results calculated by in-house code HAWTBAD.

compared to the performance results analyzed from the aerodynamic configuration designed by the in-house code.

Figure 4 shows comparison results between the experimental results and the analysis results of the Whisper H40 wind turbine. From the comparison, it is confirmed that the performance results calculated by the proposed in-house code are well agreed with average values of the experimental test results.

3. Structural design of blade

The blade loads for structural design are classified by an International Electrotechnical Commission standard (IEC). The load cases shall be determined from the combination of operational modes or other design situations, such as specific assembly, erection, or maintenance conditions, with the external conditions. All relevant load cases with a reasonable probability of occurrence shall be considered, together with the behavior of the control and protection system. According to IEC 61400-2 design requirements for small wind turbines,[20–22] total eight load cases are defined. However, this work considers three extreme load cases at normal operation, cut-off condition, and standstill and storm condition among eight load cases. Case 1 of rated wind speed condition, case 2 of cut-out wind speed condition, and case 3 of storm condition with/without gust are shown in Table 2.

Table 2. Load cases for structural design.

Load case	Case 1	Case 2	Case 3
Reference wind speed	Rated 12 m/s	Cut-out 25 m/s	Strom 55 m/s
Gust condition (±20 m/s, ±40°)	Without gust	With gust	N.A.
Rotational speed	28.2 rpm	46.9 rpm	Stop

When shear forces and bending moments are calculated along the blade span from the three load cases, it is found that the load case 2 is the highest load condition.[18,23]

Therefore, the load case 2 is considered as the structural load condition. Figure 5 shows the flapwise bending moment diagram of the load case 2.

The used materials for this work are glass/epoxy which has mechanical and economical advantages, such as proper structural strength, long fatigue life, and low cost.[24] In order to improve the structural stability as well as the lightness, glass/epoxy fabric face sheets-foam sandwich type structure is applied to the skin and the spar web. However, the spar flange carrying the major bending moments used glass/epoxy UD laminate type structure. Table 3 shows the mechanical properties of the used materials,[23] and Figure 6 shows the applied structural configuration of the blade section.

The proposed structural design procedures are as follows: initially sizing is done using the simplified design methods, and then the design is modified using the structural analysis using a FEM tool.[25]

Initial design is performed using the netting rule that the loading directional fibers can carry the design load. Then the initial design results are modified using the rule of mixture that the off-loading directional fibers can carry 10% load in addition to the major loading directional fibers. Therefore, the design results are produced with initially sized 0° directional fiber plies plus ±45° and 90° directional fiber plies.

At the initial design, the stress distribution of the spar flange is expressed as shown in Figure 7, and the flange thickness can be sized using Equations (14) and (15).

$$\sigma_{x_f} = \frac{F_x}{\sum A_i}\frac{E_{x_f}}{\bar{E}_x} + \frac{M_z(\pm y_f)}{\bar{I}_z}\frac{E_{x_f}}{\bar{E}_x} \tag{14}$$

$$\tau_{xy_f} = \frac{F_y}{\bar{I}_z}\frac{b_w}{2}\frac{b_f}{2}\frac{E_{x_f}}{\bar{E}_x} \tag{15}$$

where σ_{x_f} is the spar flange stress, F_x is the axial load, E_{x_f} is the spar flange elastic modulus, M_z is the bending moment, $\bar{E}_x$ is the equivalent elastic modulus, $\sum A_i$ is the

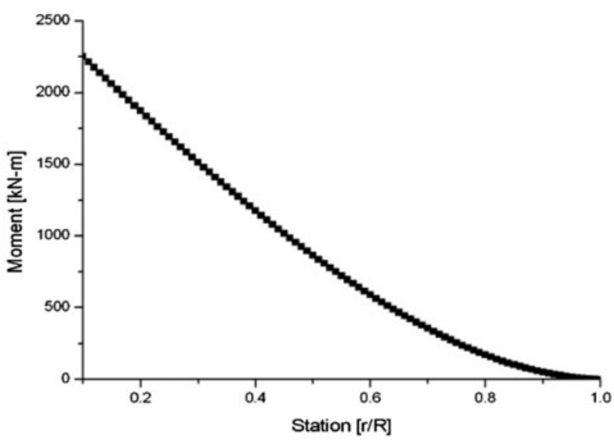

Figure 5. Flapwise bending moment diagrams of load case 2.

Table 3. Mechanical properties of materials.

Material property (N/mm^2)	UD tape GFRP	Fabric GFRP	Foam
E_1	35700	22147	60.86
E_2	10600	2658	59.86
$G_1 2$	2810	1617	19.18
ν	0.324	0.3	0.2
X_t	711	367.3	2.63
X_c	1200	411	1.41
Y_t	38	40	2.49
Y_c	183	141	1.41
S	65.7	52.8	0.71
ρ	1.8	1.87	0.1197
Ply thickness (mm)	0.58	0.3	–

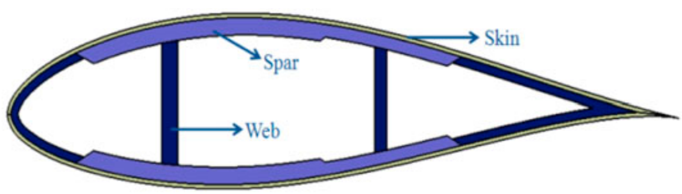

Figure 6. Conceptual structure configuration of blade cross-section.

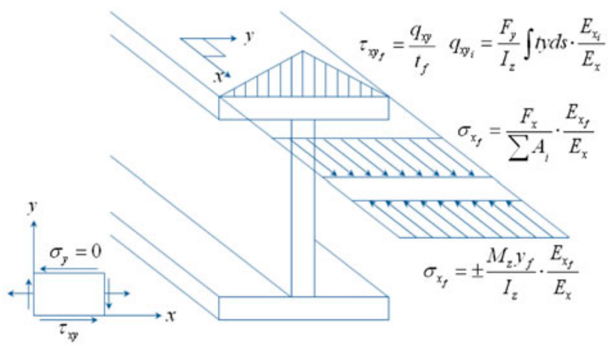

Figure 7. Acting stresses on spar flange.

cross-sectional area of spar flange and web, $\bar{I_z}$ is the second area moment of inertia of spar flange and web, τ_{xy_f} is the shear stress of spar flange, F_y is the lateral load, b_w is the web length, and b_f is the flange length.

The stress distribution of spar web is shown Figure 8, and the thickness can be sized by the normal and shear stresses as expressed in Equations (16) and (17).

$$\sigma_{x_w} = \frac{F_x}{\sum A_i} \frac{E_{x_w}}{\bar{E_x}} + \frac{M_z(\pm y_w)}{\bar{I_z}} \frac{E_{x_w}}{\bar{E_x}} \quad (16)$$

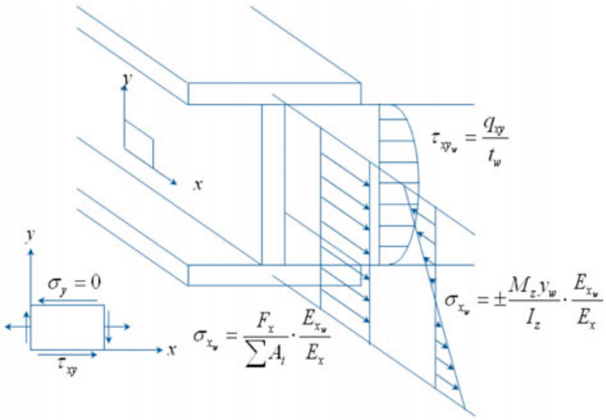

Figure 8. Acting stresses on spar web.

$$\tau_{xy_w} = 2\frac{\sigma_{x_f} t_f}{t_w} + \frac{F_y}{\bar{I}_z}\frac{b_w^2}{8}\frac{E_{x_w}}{\bar{E}_x} \quad (17)$$

where σ_{x_w} is the spar web stress, F_x is the axial load, E_{x_w} is the spar web elastic modulus, τ_{xy_w} is the shear stress of spar web, t_f is the spar flange thickness, and t_w is the spar web thickness.

Table 4. Structure design results of blade skin and spar.

Station (r/R)	Spar Front spar	Rear spar
Skin	20 plies [±455,Core,±455]	
Root–0.1	60 plies [(±45,03,90)5]s	60 plies [(±45,03,90)5]s
0.1–0.2	60 plies [(±45,03,90)5]s	40 plies [(±45,03,90)3,±45]s
0.2–0.3	66 plies [(±45,03,90)5,±45,0]s	42 plies [(±45,03,90)3,±45,0]s
0.3–0.4	74 plies [(±45,03,90)6,0]s	50 plies [(±45,03,90)4,0]s
0.4–0.5	84 plies [(±45,03,90)7]s	56 plies [(±45,03,90)4,±45,$(0)_2$]s
0.5–0.6	82 plies [(±45,03,90)6,±45,03]s	56 plies [(±45,03,90)4,±45,$(0)_2$]s
0.6–0.7	74 plies [(±45,03,90)6,0]s	48 plies [(±45,03,90)4]s
0.7–0.8	56 plies [(±45,03,90)4,±45,$(0)_2$]s	38 plies [(±45,03,90)3,0]s
0.8–0.9	36 plies [(±45,03,90)3]s	26 plies [(±45,03,90)2,0]s
0.9–1.0	20 plies [(±45,03,90),±45,$(0)_2$]s	16 plies [(±45,03,90),±45]s

Table 5. Structure design results of blade web.

Station (r/R)	Web: Front web	Web: Rear web
0.1–0.2	36 plies [±$(45)_9$,Core,±$(45)_9$]	16 plies [±$(45)_4$,Core,±$(45)_4$]
0.2–0.3	40 plies [±$(45)_{10}$,Core,±$(45)_{10}$]	16 plies [±$(45)_4$,Core,±$(45)_4$]
0.3–0.4	40 plies [±$(45)_{10}$,Core,±$(45)_{10}$]	20 plies [±$(45)_5$,Core,±$(45)_5$]
0.4–0.5	48 plies [±$(45)_{12}$,Core,±$(45)_{12}$]	20 plies [±$(45)_5$,Core,±$(45)_5$]
0.5–0.6	48 plies [±$(45)_{12}$,Core,±$(45)_{12}$]	20 plies [±$(45)_5$,Core,±$(45)_5$]
0.6–0.7	40 plies [±$(45)_{10}$,Core,±$(45)_{10}$]	20 plies [±$(45)_5$,Core,±$(45)_5$]
0.7–0.8	40 plies [±$(45)_{10}$,Core,±$(45)_{10}$]	20 plies [±$(45)_5$,Core,±$(45)_5$]
0.8–0.9	28 plies [±$(45)_7$,Core,±$(45)_7$]	16 plies [±$(45)_4$,Core,±$(45)_4$]
0.9–1.0	20 plies [±$(45)_5$,Core,±$(45)_5$]	8 plies [±$(45)_2$,Core,±$(45)_2$]

The sandwich structure is applied to improve the static structural stability as well as the lightness for both skin and web of the blade. The spar is composed of mainly 0° and 90° plies due to carrying major bending moment and additionally ±45° plies for the second directional loads and avoiding delamination by more than three layers of same directional plies. Moreover, the symmetrical lay-up is applied to remove the coupling effect between the extensional deformation and flexural deformation. The structural design results are shown in Tables 4 and 5.

4. Structural analysis of blade

To check the detail structural safety, the structural analysis is performed using a commercial finite element code, MSC. PATRAN/NASTRAN. In the analysis, the

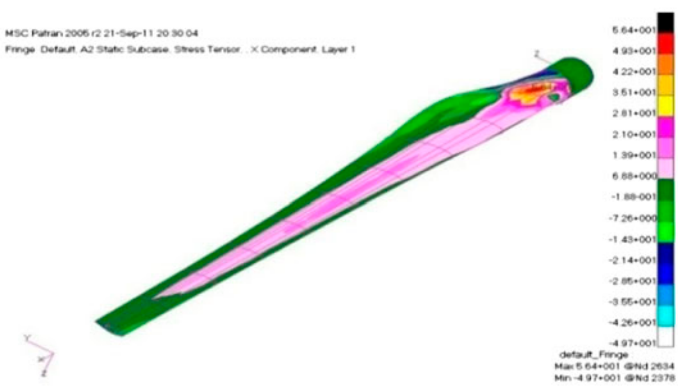

Figure 9. Spanwise stress contour on skin (1st ply).

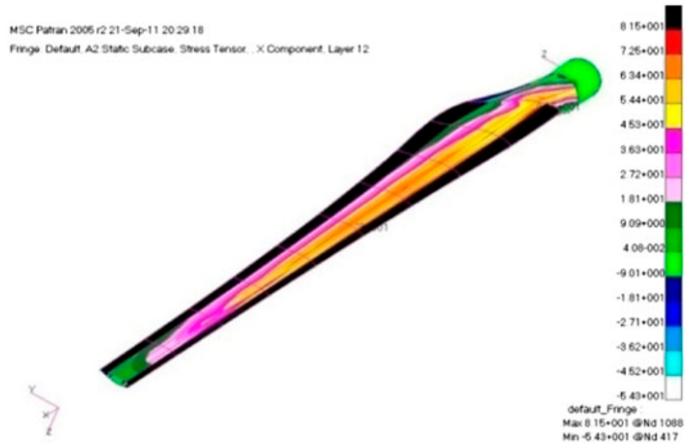

Figure 10. Spanwise stress contour on skin (21st ply).

critical design load case, in which the aerodynamic forces occurred at the cutout wind speed condition of 25 m/s with gust, is considered together with the centrifugal body force. The boundary condition of the analysis model is the fixed condition at blade root. In this analysis, the analysis results of stresses, displacements, buckling loads and modes, and natural frequencies and modes are investigated.[25,26]

Two kinds of core materials, i.e. urethane foam and balsa wood of the sandwich structure applied to both skin and spar web, are considered to find a much lighter blade.[27] According to comparison results, in case of the urethane foam core sandwich, the maximum tensile and compressive stresses of the skin (1st ply) are 56.4 and 49.7 MPa, respectively, the tensile and compressive stresses of the spar flange (21th ply) are 54.3 and 81.5 MPa, respectively, the deflection of the blade tip is 2.94 m, and the structure weight is 4.32 tonnes. In case of the balsa core sandwich, the stress distribution and the blade tip deflection are similar to the urethane foam core sandwich

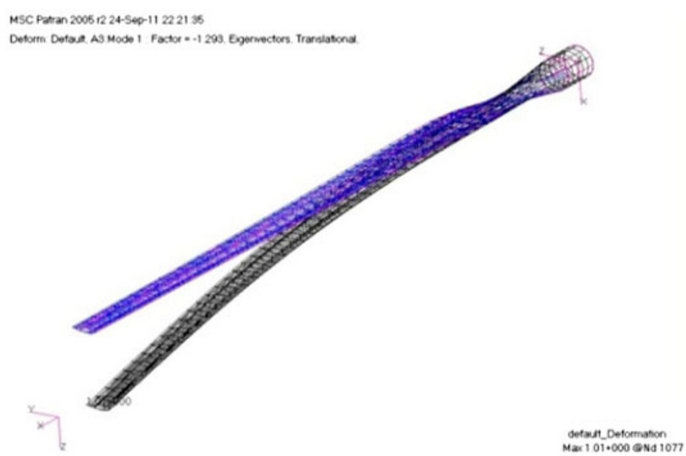

Figure 11. First buckling mode shape and load factor.

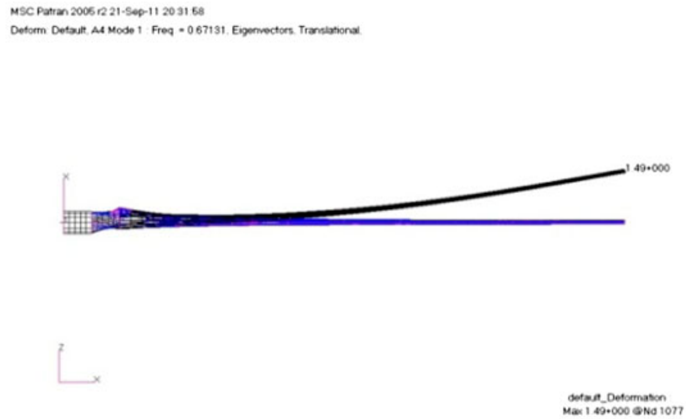

Figure 12. First flapwise mode shape and natural frequency.

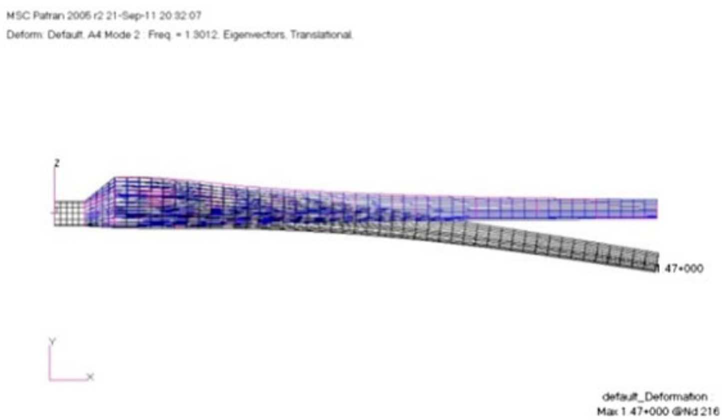

Figure 13. First chordwise mode shape and natural frequency.

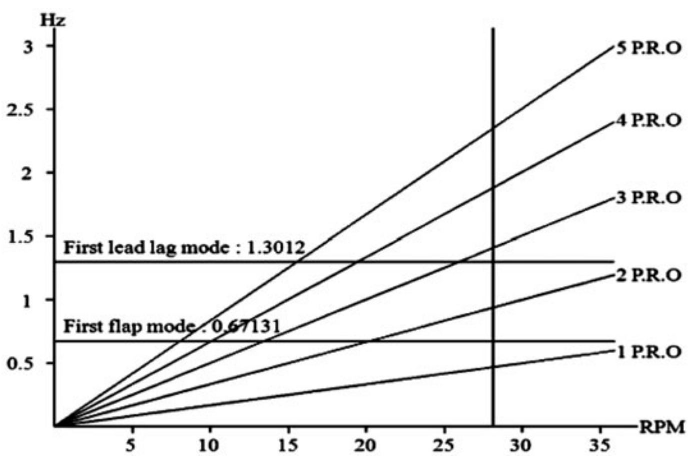

Figure 14. Campbell diagram.

case, but the structure weight is 5.04 tonnes. Therefore, the urethane foam core sandwich structure is finally selected, and it is a bit lighter than the existing same MW class commercial wind turbine blade, UGE 1000H of ETC Green Co. having 4.35 tonnes weight.

The buckling load factors of the finally selected blade are 1.293 at the first mode and 4.093 at the second mode, respectively, and it means that the blade is safe for the static structural stability. Moreover, the natural frequencies and modes of the blade are analyzed, and the resonance possibility is investigated by Campbell diagram. From this investigation, it is found that the proposed blade is safe from the resonance.

Figures 9 and 10 show the spanwise stress contour on skin and spar, and Figure 11 shows the first buckling mode shape and load factor. Figures 12 and 13 show the first flapwise and chordwise mode shapes and natural frequencies. Figure 14 shows the Campbell diagram to examine the resonance possibility.

5. Fatigue life estimation of blade

Wind turbine blade structural design requirements include generally three important requirements such as limit strength, stiffness, and fatigue life. In order to satisfy the limit strength requirement, the blade structure should endure not only the maximum load that may occur during operation but also be safe at storm as well as gust. The stiffness requirement means that the blade should have a proper stiffness to avoid the resonance, an enough stiffness to prevent the blade tip's hitting to the tower wall, and an enough torsional stiffness to minimize the torsional deformation that may change the aerodynamic performance.

Finally, the fatigue life requirement means that the blade should endure the repeated fatigue loads until the required fatigue life.

In this work, using experimental fatigue load spectrums obtained from a similar wind turbine system and Mandell's S–N diagram and Goodman diagram of applying composite materials, the required maximum fatigue strength is firstly calculated and then the fatigue life is estimated using the modified Spera's formulae.[5] The dynamic structural problem for the fatigue analysis can be converted into the static structural problem.[23]

Mandell's S–N experimental approximation equation having stress ratio of 0.1 for the UD glass/epoxy composite laminate is expressed by [5].

$$S/S_0 = N_f^{-0.074} \tag{18}$$

where S/S_0 is the normalized stress, S_0 is the strength of the used materials, and N_f is the number of fatigue cycles.

From the measured load spectrum of the 2.5 MW class wind turbine NASA/DOE Mod-2's blade as shown in Figure 15, the average stress ratio (R_{avg}) was calculated as 0.37. To compensate the average stress ratio R_{avg} to an arbitrary stress ratio R, Goodman diagram as shown in Figure 16 is used, the slope from the following equation is used to obtain S_{max} and S_{min} at 10^8 cycles.[23]

$$S_{cyc}/S_{avg} = (1 - R)/(1 + R) \tag{19}$$

where S_{cyc} is $(S_{max} - S_{min})/2$, and S_{avg} is $(S_{max} + S_{min})/2$.

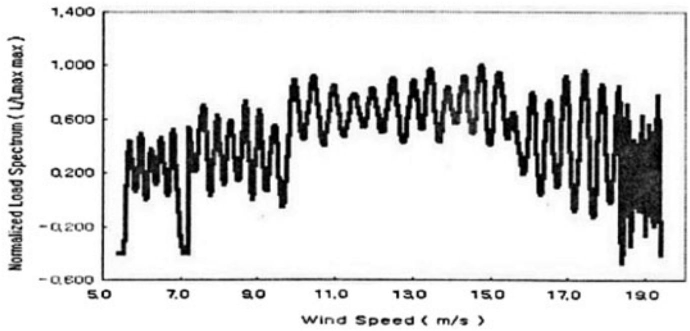

Figure 15. Measured load spectrum of NASA/DOE Mod-2 wind turbine blade.

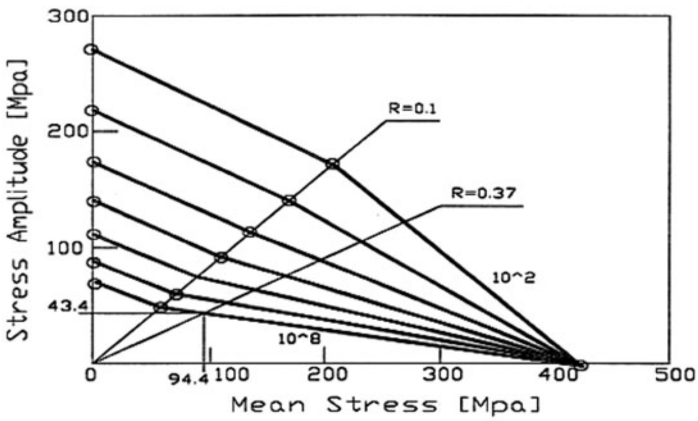

Figure 16. Goodman diagram of glass/epoxy composite materials.

To calculate S'_{max} for the required fatigue life from S_{max}, the following Mandell's equation is used.

$$S'_{max} = S_{max} \times N_f^{-0.074} \times (1/10^8)^{-0.074} \tag{20}$$

The 20-year fatigue cycles can be calculated by extending the measured spectrum for 9 h using the following equation.

$$N_f = 20\,\text{yr} \times 8760\,\frac{\text{hr}}{\text{yr}} \times \frac{\text{No. of cycle test}}{\text{Test duration(hr)}} \tag{21}$$

The allowable fatigue stress using the S–N linear damage method is obtained by the following equation.[5,23]

$$S_{\max\,\max} = S_I \left[N_f \frac{\sum_{i=1}^{n} n_i R_i^{13.5}}{\sum_{i=1}^{n} n_i} \right]^{-0.074} \tag{22}$$

where n is the total layer number and n_i is the cycle number of each layer.

To apply the calculated allowable fatigue stress to the actual rotating blade, the knock down factor (KDF) less than one must be used. This work uses KDF of 0.7

Table 6. Estimated allowable fatigue stresses.

N_f	S_{max}	S_I	$S_{max\ max}$	$S_{max\ max} \times KD$
3.72×10^8	230 MPa	790 MPa	218.8 MPa	153.2 MPa

based on the existing similar class wind turbine blade. Table 6 shows the calculation result of allowable required fatigue strength, 153.2 MPa.[15,23]

The fatigue of the rotating blade is caused by several reasons, i.e. different rotating axis from wind direction, change of wind speed, gravitational blade loading change due to rotating, etc.

The cyclic load, which affects the blade fatigue life, is divided into the flapwise load and the chordwise load. The flapwise and chordwise cyclic loads can be calculated using the following modified Spera's empirical formula.[15,16]

$$\Delta M_{y,n} = aM_g \sin\theta + 432(1 + 1.47a) \times cd(g + 0.012b) \times U_n(1 - s) \times \exp^{(0.134n)}(D/100)^4 \tag{23}$$

$$\delta M_{z,n} = eM_g + 46.8cd(g + 0.01b) \times U_n(1 - s)\exp^{(0.276n)}(D/100)^3 \tag{24}$$

where δM_y is the blade cyclic flapwise bending load, δM_z is the blade chordwise bending load, n is the number of standard deviations, a is the hub-rigidity factor, b is the tower blockage factor, c is the tip chord factor, d is the air density factor, e is the chordwise dynamic amplification factor, f is the flapwise dynamic amplification factor, g is the wind variation factor, D is the rotor diameter, M_g is the blade maximum static gravity moment, θ the hub coning angle, U_n is the wind speed at hub elevation, and s is the blade station.

In order to obtain $M_{y,n}$ max and $M_{z,n}$ max, the estimated cyclic loads of $\delta M_{y,n}, \delta M_{z,n}$, and the average R-ratio obtained from the fatigue load spectrum are used. In this work, the type II ($n = 2$, 2% probability exceedance) fatigue loads of $M_{y,n}$ max

Figure 17. Spanwise stress contour on spar (21th ply) due to type II fatigue loads.

and $M_{z,n}$ max are used for calculating the fatigue stresses using the finite element method.

According to stress analysis results, maximum compressive and tensile stresses are −73.1 and 76.1 MPa, respectively. Figure 17 shows stress contour at maximum type II fatigue loads.

However, because the allowable fatigue stress for 20 years fatigue life is 153.2 MPa, the calculated fatigue stresses due to the type II fatigue loads are relatively quite low. Therefore, it is confirmed that the designed wind turbine blade has enough fatigue life more than the required 20 years fatigue life.

6. Conclusions

This work is to establish the proper design procedure as well as to design the high efficiency and lightweight 1 MW class horizontal axis wind turbine blade considering more than 20 years fatigue life.

The blade aerodynamic configuration is induced considering the design requirements, and it is found that the proposed wind turbine blade has better performance than the existing commercial wind turbine blade.

Through the trade-off study, the skin-spar-foam sandwich composite structure is adopted. The glass/epoxy fabric face sheet-urethane foam core sandwich structure for both skin and spar web and the glass/epoxy UD laminate structure for spar flange are used to give proper structural strength, better static structural stability, low cost, and lightness.

The structural design is performed by the load case study, the initial sizing using the netting rule and the rule of mixture, and the design modification using FEM analysis.

The structural safety of the finally proposed blade is confirmed by analyzing the stresses, the deformations, the buckling load factors, the natural frequencies, the Campbell diagram, etc. It is found that the proposed blade is a bit lighter than the existing commercial blade.

Fatigue loads, such as flapwise and chordwise bending moments are calculated by Spera's empirical equations with various engineering data and probability of exceeding. And the allowable fatigue stress for the required design life is estimated from the S–N curve of glass/epoxy laminate by Mandell's empirical equations and Goodman diagram with the modified stress ratio. It is confirmed that the designed blade has enough fatigue life of over 20 years.

Acknowledgment

This work was supported by research funds from Chosun University, 2013.

References

[1] Dincer F. The analysis on wind energy electricity generation status, potential and policies in the world. Renewable Sustainable Energy Rev. 2011;15:5135–5142.

[2] Grujicic M, Arakere G, Subramanian E, Sellappan V, Valejo A, Ozen M. Structural-response analysis, fatigue-life prediction and material selection for 1 MW horizontal-axis wind-turbine blades. J. Mater. Eng. Perform. 2012;19:790–801.

[3] Sun P, Liu Z, Gao Y, Wu S. Lay-up design and structural analysis of 1.2 MW composite wind turbine blade. In: Proceeding of IEEE 10th International Conference on CACID & CD. Wenzhou: Wenzhou University, China. 2009. p. 73–76.

[4] Jang M, Bang H. The current status and the prospects of wind energy. J. Environ. Sci. 2009;18:933–940.
[5] Spera DA. Dynamic loads in horizontal axis wind turbines part: empirical equations. Wind power; 1993.
[6] Palmgren A. Die Lebendauer von Kugellagern [The lifetime of ball bearings]. Zeitschrift von Deutche Ingenieurring. 1924;68:339–341.
[7] Miner MA. Cumulative damage in fatigue. J. Appl. Mech. 1945;12:A-159–164.
[8] Mandell JF, Reed RM, Samborsky DD. Fatigue of fiberglass wind turbine blade materials. SAND92-7005. Albuquerque (NM): Sandia National Laboratories; 1992.
[9] Veers PS, Lange CH, Winterstein SR. Farow: a tool for fatigue and reliability of wind turbines. In: Windpower'93; 1993; San Francisco, CA. p. 342–349.
[10] Bishop NWM, Zhihua H. The fatigue analysis of wind turbine blades using frequency domain techniques. In: EWEC'91; Amsterdam; 1991.
[11] Broek D. Elementary engineering fracture mechanics. Martinus Nijhoff Publishers; 1982.
[12] Tada H, Paris PC, Irwin GR. The stress analysis of cracks handbook. Paris Productions Inc.; 1985.
[13] Suresh S. Fatigue of materials. Cambridge University Press; 1991.
[14] Finger RW. Methodology for fatigue analysis of wind turbines. In: Proceeding Windpower'85 Conference; 1985; San Francisco, CA. p. 52–56.
[15] Kong C, Kim T, Han D, Sugiyama Y. Investigation of fatigue life for a medium scale composite wind turbine blade. Int. J. Fatigue. 2006;28:1382–1388.
[16] Kong C, Bang J, Sugiyama Y. Structural Investigation of composite wind turbine blade considering various load cases and fatigue life. Energy. 2005;30:2101–2114.
[17] Gourieres DL. Wind power plants. Pergamon Press; 1982.
[18] Kong C, Park H, Choi S. Study on a 500 W class wind turbine using a high efficiency composite blades. J. KSAS. 2009;37:201–208.
[19] Frank B, Niels S, Jeppe J, Peter F. Wind turbine airfoil catalogue. Riso National Laboratory; 2001.
[20] IEC International Standard. Wind turbine generator system Section 415-02: Design and safety parameters; 1994.
[21] International Standard IEC 61400-1. 2005;21–32.
[22] Lloyd G. Regulations for the certification of wind energy conversion system. Germanischer Lloyd; 1999.
[23] Kong C. Structural design of medium scale composite wind turbine blade. KSAS Int. J. 2001;1:92–102.
[24] Farrow I. R. An introduction to composite materials. Bristol University; 1997.
[25] Kong C, Choi S, Park H. Investigation on design for a 500 W wind turbine composite blade considering impact damage. Adv. Compos. Mater. 2000;72:524–573.
[26] MSC Software. MSC. Patran 2002 reference manual; 2000.
[27] DIAB ProBalsa ® HW heavy weight balsa wood. Available from: http://www.Matweb.com